

# Dynamical dislocation lines in the charge density wave systems

---

Jelčić, Dajana; Bjeliš, Aleksa

Source / Izvornik: **Fizika A**, 1992, 1, 93 - 109

Journal article, Published version

Rad u časopisu, Objavljena verzija rada (izdavačev PDF)

Permanent link / Trajna poveznica: <https://um.nsk.hr/um:nbn:hr:217:911232>

Rights / Prava: [In copyright](#) / [Zaštićeno autorskim pravom.](#)

Download date / Datum preuzimanja: **2025-03-26**



Repository / Repozitorij:

[Repository of the Faculty of Science - University of Zagreb](#)



## DYNAMICAL DISLOCATION LINES IN THE CHARGE DENSITY WAVE SYSTEMS

DAJANA JELČIĆ and ALEKSA BJELIŠ

*Department of Physics, Faculty of Science, University of Zagreb, P. O. B. 162,  
41001 Zagreb, Croatia*

Received 8 March 1992

UDC 538.93

Original scientific paper

The topological aspects of the conversion of collective charge density wave transport into the ohmic one in front of extended barriers are discussed in the frame of Gor'kov's model. It is shown that simultaneous phase slips form a family of dislocation lines. The shape and dynamics of these lines depend on the morphology of the barrier. They influence the amplitude of the narrow band noise, but do not modify its fundamental frequency.

### 1. Introduction

The Peierls ground state<sup>1)</sup>, one of the possible low-temperature broken symmetries which characterize quasi-one-dimensional systems, is a periodic deformation of the ionic lattice, accompanied with the formation of the electronic charge density wave (CDW). In an ideal crystal lattice, the energy of the electron-ion system does not depend on the phase of the CDW, while the gap in the electron spectrum, which opens at the Fermi level, prevents the low-energy single particle excitations. The CDW should therefore slide without dissipation under the influence of the external electric field, exhibiting the so called Fröhlich superconductivity<sup>2)</sup>.

The CDW has been found by now in few classes of materials<sup>3)</sup>, but the behaviour which resembles to the Fröhlich superconductivity has been observed only in some experiments<sup>4)</sup> on the blue bronze  $\text{K}_{0.3}\text{MoO}_3$  at very high electric fields and well below the temperature of the phase transition. Otherwise, one encounters the collective dissipative flow of CDW which starts above a finite threshold electric field, characterizing a particular system.

A remarkable property of the collective CDW transport is the generation of multiharmonic voltage oscillations, usually called the narrow band noise (NBN)<sup>3)</sup>. The fundamental frequency of the NBN is proportional to the collective current, i.e. to the CDW velocity. The spectral lines are narrow, but still finite, suggesting the spatial distribution of the CDW velocities within the system. Some experiments show that the NBN amplitude varies also in time, on scales much longer than the NBN periodicity<sup>5,6)</sup>. Similar conclusions follow also from the broad band noise (BBN), the low frequency oscillations which appear simultaneously with the NBN. The characteristic  $1/f$  dependence of the BBN amplitude on frequency implies the spatial and/or temporal inhomogeneities of the CDW velocity within the sample<sup>6)</sup>.

A lot of theoretical work was devoted to the mechanisms which disturb the perfect Fröhlich superconductivity<sup>7)</sup>, and cause the above experimental findings. One of the most obvious comes from the impurities and/or other sample defects. They destroy the translational invariance of a system, which is the basic condition for the Fröhlich superconductivity. The specific mechanism by which the CDW interacts with impurities and, in particular, the effects of impurities on the CDW dynamics and the NBN generation above the threshold electric field, remain however still controversial to some extent. At present, the theoretical interpretations of these effects point into two main directions.

The first one is concerned with the effects of so called weak impurities, which are randomly distributed within the bulk of the specimen. The individual strength of weak impurities is not sufficient to stop locally the CDW transport. It was however pointed out by Fukuyama, Lee and Rice (FLR)<sup>8,9)</sup>, that the cooperative action of sufficiently dense weak impurities can pin the CDW phase within the phase coherent domains, at lengths much larger than the corresponding correlation lengths.

It is by now well accepted that the FLR weak pinning is responsible, at least partially, for the finite threshold field. This approach became also a basis for a variety of so called bulk models<sup>10–13)</sup> for the CDW dynamics above the threshold. The main assumption of these models is that the CDW deformations due to the weak impurities are approximately elastic. While the energy of the long wavelength phase excitations can be arbitrary low, the energy of the amplitude fluctuations is of the order of the CDW condensation energy and thus much higher than the weak-pinning energy. The amplitude excitations are therefore neglected within these models, and the CDW is considered as an elastic medium having only the phase degrees of freedom. The variations of the order parameter on the microscopic scales due to the interaction of the CDW phase with weak bulk impurities is then usually substituted by some effective phenomenological potential which reflects the periodicity of the CDW itself. The temporal modulations of the bulk CDW velocity due to this potential are expected to be responsible for the generation of the NBN.

An alternative approach to the CDW dynamics invokes strong and isolated crystal defects, for example the ohmic contacts, sample and grain boundaries, etc. At such places the CDW transport is partially or completely suppressed, i. e. the CDW velocity passes through sharp discontinuities. Different phase winding rates in regions with different velocities, would cause the boundless accumulation

of electronic charge. This can be prevented only by a local conversion of the CDW current into the ohmic one. Gor'kov<sup>14)</sup> proposed that this conversion proceeds through phase-slippages (PS) in the vicinity of strong defects. The process of PS had been originally invoked for the explanation of the finite resistivity in thin superconducting fibers<sup>15,16)</sup>. It is a fast and localized annihilation of the order parameter amplitude, during which its phase slips by  $2\pi$ . Thus on the contrary to the "phase only" models, the PS models take into account fast and localized CDW deformations, including the amplitude degrees of freedom. The NBN is attributed just to these deformations.

In the first microscopic analysis of the PS process in the CDW, Gor'kov considered the limit of so called dirty systems<sup>14)</sup>, i.e. systems with very short relaxation times for band electrons. The problem can be then reduced to a diffusion equation of Ginzburg-Landau type. The detailed analytical<sup>14)</sup> and numerical<sup>17,19)</sup> treatments of this equation in the one-dimensional case led to qualitative, and sometimes quantitative explanations of NBN and some other effects linked to the CDW dynamics. It was also shown<sup>20)</sup> that the spatial variations of the external electric field lead to the appearance of finite numbers of dynamical domains with different mean velocities, and correspondingly, to the PS generation in the bulk of the specimen.

The opposite case of clean CDW systems, i. e. long electron relaxation times, was addressed by Artemenko et al.<sup>21)</sup>. Due to the long range correlations in this limit it is not possible to formulate a local equation of motion. PSs have to be treated on quantum level, as amplitude solitons with adiabatic dynamics. The main physical consequences are however the same as in Gor'kov's limit.

Although the PS model is in both limits<sup>14,21)</sup> formulated for a three-dimensional system, the analyses were up to now limited mostly to the one-dimensional solutions. On the other hand, Ong and Maki<sup>22)</sup> proposed that the conversion of the CDW current occurs through the formation of phase vortices in front of strong barriers. They used the vortex solution of the static Landau equation for the complex order parameter and imposed phenomenologically their transverse motion in order to ensure the evacuation of accumulated charge. Similar model of static elastic medium was considered by Feinberg and Friedel<sup>23)</sup> who established the analogy of CDW vortices and dislocation lines in the three-dimensional crystal lattice, and analyzed the role of these lines in the depinning of CDW in front of the barrier.

In this paper we show that the Ginzburg-Landau diffusion equation has a special type of three-dimensional solutions, dynamic phase vortices, i.e. dislocation lines. These dislocation lines are shown to be a 3D generalization of the one-dimensional PS centers. In fact, the core of our dislocation lines is an array of simultaneous PS centers. We also show that the motion of dynamical dislocation lines depends on the details of boundary conditions imposed by the transverse barrier. This possibility was already mentioned in Ref. 14, and partially elaborated in Refs. 24 and 25. Here we extend the analysis by undertaking the thorough numerical analysis, and discussing the effects of chain discreteness and lateral sample boundaries.

The Gor'kov's model and the corresponding description of the PS process in the one-dimensional system is shortly reviewed in Sect. 2. This description is ex-

tended in Sect. 3. to dynamical dislocation lines as the solutions of the problem with a flat transverse barrier and general boundary conditions. In Sect. 4 we consider the particular example of boundary condition with the linearly varying CDW phase in one transverse direction. We obtain a train of moving dislocation lines, in correspondence with the phenomenological picture of Ref. 22. The limitations and possible generalizations of our results are discussed in the concluding Sect. 5.

## 2. Gor'kov's model

Under the circumstances specified in the Introduction, the collective CDW dynamics follows from the Landau type of equation<sup>14)</sup>,

$$\frac{\partial \Delta}{\partial t} = \frac{\partial^2 \Delta}{\partial \mathbf{r}_\perp^2} + \frac{\partial^2 \Delta}{\partial x^2} + \Delta - |\Delta|^2 \Delta - iE\Delta, \quad (1)$$

for the complex CDW order parameter  $\Delta = |\Delta(\mathbf{r}, t)| \exp(i\Phi(\mathbf{r}, t))$ . Here  $|\Delta|$  is measured in terms of its thermodynamic value  $|\Delta_\infty|^2 = (6/5)\pi^2 T_P^2 \delta$ , where  $\delta \equiv 1 - T^2/T_P^2$ , and  $T_P$  is the temperature of the Peierls phase transition. As already mentioned, in the region of applicability of Gor'kov's equation the concentrations of impurities are close to the critical one, above which the Peierls phase transition would be completely suppressed. Therefore  $T_P \ll T_P^0$ , where  $T_P^0$  is the Peierls temperature in absence of impurities. The length and time scales are defined by the correlation lengths  $\xi_{x,\perp}$  and the characteristic frequency  $\omega_0 \equiv (10/27)|\Delta_\infty|^2 \tau_c$ , respectively. Here  $\tau_c = 4\gamma/3\pi T_P^0$ , where  $\gamma$  is the Euler constant, and  $\tau_c$  corresponds to the critical relaxation time for the normal electrons. The unit of the electric field  $E$  is defined by the condition  $eEv_F = (5/36)|\Delta_\infty|^2$ .

Equation (1) has a simple particular solution

$$\Delta(\mathbf{r}, t) = \exp(-iEt), \quad (2)$$

which represents the uniform CDW motion with a velocity proportional to the constant external electric field. The presence of various inhomogeneities disturbs, i.e. slows down or even completely stops, this flow. In the Gor'kov's approach (1), the weak and smooth disturbances of this kind are neglected, the only exception being the possible spatial variations of the electric field  $E(\mathbf{r})$ . This approximation is justified for  $E(\mathbf{r}) \gg E_T$ , where  $E_T$  is the bulk threshold field caused by the finite concentration of weak impurities inside the sample. On the other hand, the effects of strong obstacles enter into the problem (1) through the appropriate boundary conditions. E.g., the local stoppage of the CDW is modeled by imposing the static value of  $\Delta$  at the obstacle.

The simple example of this kind is the CDW flow in the semi-infinite geometry, with the static value

$$\Delta(x=0, \mathbf{r}_\perp) = \Delta(x=0) = \Delta_0 \quad (3)$$

at the planar transversal boundary. Then the problem (1) allows for a particular solution  $\Delta(x, t)$  which does not vary transversally. As was shown numerically<sup>17)</sup>,  $\Delta(x, t)$  comprises planar PSs, which occur periodically in time with the period equal to  $2\pi/E$  in reduced units. At the moment of PS, the amplitude of the CDW collapses at  $x_{PS} \approx E^{-0.284}$ , while its phase simultaneously slips for  $2\pi$ , which enables the conversion of charge from the CDW condensate to the ohmic carriers. The diffusion of minimum in  $\Delta(x, t)$  resulting in the PS, is a nonlinear process, with a characteristic space scale defined by  $x_{PS}$ . It is responsible for the additional local variation of the electric field<sup>14)</sup>

$$\delta E(\mathbf{r}, t) = \lambda \left\{ |\Delta|^2 E - \frac{16}{9} \varepsilon |\Delta|^2 \dot{\Phi} \right\}, \quad (4)$$

where

$$\varepsilon = \frac{\bar{v}_F^2}{(v_F^2)} \approx 1, \quad \lambda \equiv \frac{8}{3} (\Delta_\infty \tau_c)^2 \ll 1. \quad (5)$$

The corresponding contribution to the sample voltage

$$V(t) = \int \delta E d\mathbf{r} \quad (6)$$

is in the presence of constant external electric drive  $E$  periodic, highly nonsinusoidal<sup>17)</sup> and, as such, is a possible source of NBN.

### 3. General solution for dynamical dislocation lines

Let us now generalize the boundary condition (3) by allowing the transverse dependence of  $\Delta(x = 0, \mathbf{r}_\perp)$ ,

$$\Delta(x = 0, \mathbf{r}_\perp; t) = \Delta_0(\mathbf{r}_\perp). \quad (7)$$

The corresponding solution  $\Delta(\mathbf{r}, t)$  depends now on all three space coordinates, so that the numerical integration becomes very complicated. We continue instead by using an approximate analytical method justifiable in the asymptotic limit of large electrical fields,  $E \gg 1$ <sup>14,17,18)</sup>. The previous analytical and numerical results, concerning the one-dimensional CDW dynamics, show that in this limit one loses some important quantitative properties of the PS diffusion, in particular the multiharmonicity of the NBN. In this work we are however mainly concerned with the qualitative topological aspects of the PS process, which are independent of the value of  $E$ . The results valid in the regime  $E \gg 1$  are therefore sufficient for our purposes.

The PSs appear due to the matching of the local, almost static variations of  $\Delta(\mathbf{r}, t)$  close to the boundary at  $x = 0$ , and the uniform CDW flow (2) far from the

boundary. We assign, respectively, to each region the functions  $\Delta_L$  and  $\Delta_R$ , which satisfy the conditions

$$\begin{aligned}\Delta_L(x \rightarrow \infty) &= 0, \\ \Delta_R(x = 0) &= 0,\end{aligned}\tag{8}$$

and assume that the total solution of Eqs. (1, 7) is of the form

$$\Delta(\mathbf{r}, t) = \Delta_L(x, \mathbf{r}_\perp) + \Delta_R(x, t).\tag{9}$$

The bulk part  $\Delta_R$  should be insensitive to the boundary condition (7) and therefore  $\mathbf{r}_\perp$ -independent. The exact particular solution of Eq. (1), satisfying the condition (8) is

$$\Delta_R(\mathbf{r}, t) = \tanh \frac{x}{\sqrt{2}} e^{-iEt}.\tag{10}$$

On the other hand, the part  $\Delta_L$  has to satisfy both Eq. (1) and the boundary conditions (7) and (8). The former is simplified after neglecting the weak time dependence of  $\Delta_L$ , i.e. the term  $\dot{\Delta}_L$ , and the potential part  $\Delta_L - |\Delta_L|^2 \Delta_L$  due to the relative predominance of the term  $iE\Delta_L$  when  $E \gg 1$ . Equation (1) then reduces to the linear equation

$$\frac{\partial^2 \Delta_L}{\partial \mathbf{r}_\perp^2} + \frac{\partial^2 \Delta_L}{\partial x^2} \approx iE\Delta_L.\tag{11}$$

Taking into account the conditions (7) and (8), and passing to the Fourier transform of Eq. (11) with respect to  $\mathbf{r}_\perp$ , one gets the solution in the integral form,

$$\begin{aligned}\Delta_L(x, \mathbf{r}_\perp) &= \frac{1}{(2\pi)^2} \int d^2 \mathbf{r}'_\perp \int d^2 q_\perp \Delta_0(\mathbf{r}'_\perp) \exp(i\mathbf{q} \cdot (\mathbf{r}_\perp - \mathbf{r}'_\perp)) \\ &\quad - \sqrt{\frac{1}{2}(q_\perp^2 + \sqrt{q_\perp^4 + E^2})} x - \text{sgn}(E) \sqrt{\frac{1}{2}(-q_\perp^2 + \sqrt{q_\perp^4 + E^2})} x.\end{aligned}\tag{12}$$

The places and moments of PSs are determined by the condition

$$\Delta(x_{ps} \bar{\mathbf{r}}_\perp^{ps}, t_{ps}) = 0,\tag{13}$$

i.e. by

$$|\Delta_L(x_{ps} \bar{\mathbf{r}}_\perp^{ps})| = \tanh \frac{x_{ps}}{\sqrt{2}},\tag{14a}$$

$$\Phi_L(x_{ps}, \mathbf{r}_\perp^{ps}) + Et_{ps} = (2n + 1)\pi \text{sgn}(E),\tag{14b}$$

where  $\Delta_L \equiv |\Delta_L| \exp(i\Phi_L)$ .

Equation (14a) defines a PS surface  $x_{ps}(\mathbf{r}_\perp)$  at which the PSs occur. In the case of the boundary conditions (3) this was a plain at distance  $x_{ps}$  from the boundary at  $x = 0$ . The intersection of the surface  $x_{ps}(\mathbf{r}_\perp)$  with the set of equiphase surfaces differing in phase by  $2\pi$ , defined by the condition (14b), determines the family of continuous curves at which the PSs occur simultaneously at a given time  $t_{ps}$ , i. e. the family of dislocation lines. The motion of each dislocation line on the surface  $x_{ps}(\mathbf{r}_\perp)$  is determined by a velocity in a direction orthogonal to the equiphase line at a given point  $\mathbf{r}_\perp$ ,

$$v_\Phi(\mathbf{r}_{ps}(t)) = -\frac{E}{|\Delta\Phi_L|_{\mathbf{r}=\mathbf{r}_{ps}}} . \quad (15)$$

As is evident from Eqs. (14a, b, 15), the shape and dynamics of dislocation lines depend on the functions  $|\Delta_L\mathbf{r}|$  and  $\Phi_L(\mathbf{r})$ , i.e. via Eq. (12) on the function  $\Delta_0(\mathbf{r}_\perp)$  which specifies the boundary condition (7). On the contrary, the time interval between two PSs at a given point of  $x_{ps}(\mathbf{r}_\perp)$  is independent of  $\Delta_0(\mathbf{r}_\perp)$ , and is given by

$$t_{ps}^{n+1} - t_{ps}^n = \frac{2\pi}{E} . \quad (16)$$

In other words, the transversal  $\Delta_L$  dependence does not influence the fundamental PS periodicity at a given  $\mathbf{r}_\perp$  (i.e. chain), but only time shifts between the PSs at different chains. This influences also the PS voltage. The time dependent part of the expression (6) for the solution of the form (9) reads as

$$\begin{aligned} \delta V(t) &\sim \int dx \int d\mathbf{r}_\perp |\Delta_L(x, \mathbf{r}_\perp)| \tanh \frac{x}{\sqrt{2}} \cos(Et + \Phi_L(x, \mathbf{r}_\perp)) \\ &\approx \int d\mathbf{r}_\perp |\Delta_L(x_{ps}(\mathbf{r}_\perp), \mathbf{r}_\perp)|^2 \cos(E(t - t_{ps}(\mathbf{r}_\perp))) , \end{aligned} \quad (17)$$

where in the second line we have taken into account that  $\Delta_L$  and  $\Delta_R$  overlap appreciably only in the narrow PS region. The frequency of NBN is thus not influenced by the transverse motion of dislocation lines. However, a continuous distribution of  $t_{ps}(\mathbf{r}_\perp)$  throughout the sample cross section may lead to a reduction, or even to an annihilation, of the overall NBN amplitude with respect to the planar condition (3).

#### 4. *Straight dislocation lines*

To illustrate the above conclusions we choose a simple boundary condition

$$\Delta_0(\mathbf{r}_\perp) = |\Delta_0| \exp(iQy) , \quad (18)$$

where  $y$  is the transverse rectilinear coordinate and  $Q$  and  $|\Delta_0|$  are real constants. The straightforward integration of Eq. (12), with the condition (18) taken into



account, leads to the result

$$\Delta_L(Q, E; x, y) = |\Delta_0| \exp[iQy + (i\alpha - \beta)x], \quad (19)$$

with

$$\alpha = -\operatorname{sgn}(E) \sqrt{\frac{1}{2}(-Q^2 + \sqrt{Q^4 + E^2})},$$

$$\beta = \sqrt{\frac{1}{2}(Q^2 + \sqrt{Q^4 + E^2})}. \quad (20)$$

The corresponding conditions defining the PS dislocation lines are

$$|\Delta_0| e^{-\beta x_{ps}} = \tanh \frac{x_{ps}}{\sqrt{2}}, \quad (21a)$$

$$\alpha x_{ps} + Q y_{ps} + E t_{ps}^n = (2n + 1)\pi \operatorname{sgn}(E). \quad (21b)$$

As follows from Eq. (21a), the surface  $x_{ps}(\mathbf{r}_\perp)$  is a plane parallel to the boundary at  $x = 0$ , positioned at the distance

$$x_{ps}(y, z) \approx \frac{1}{\beta} \ln(\sqrt{2} |\Delta_0| \beta). \quad (22)$$

The geometrical form of simultaneous PSs in this plain is a train of parallel straight dislocation lines in the  $z$ -direction, defined by

$$y_{ps}(t_{ps}) = -\frac{E}{Q} t_{ps} + \frac{2n\pi}{Q} \operatorname{sgn}(E) + \text{const.} \quad (23)$$

The distance between two neighbouring lines is

$$D = \frac{2\pi}{Q}. \quad (24)$$

The dislocation lines travel along the  $y$ -axes with a constant velocity

$$v_y = -\frac{E}{Q}. \quad (25)$$

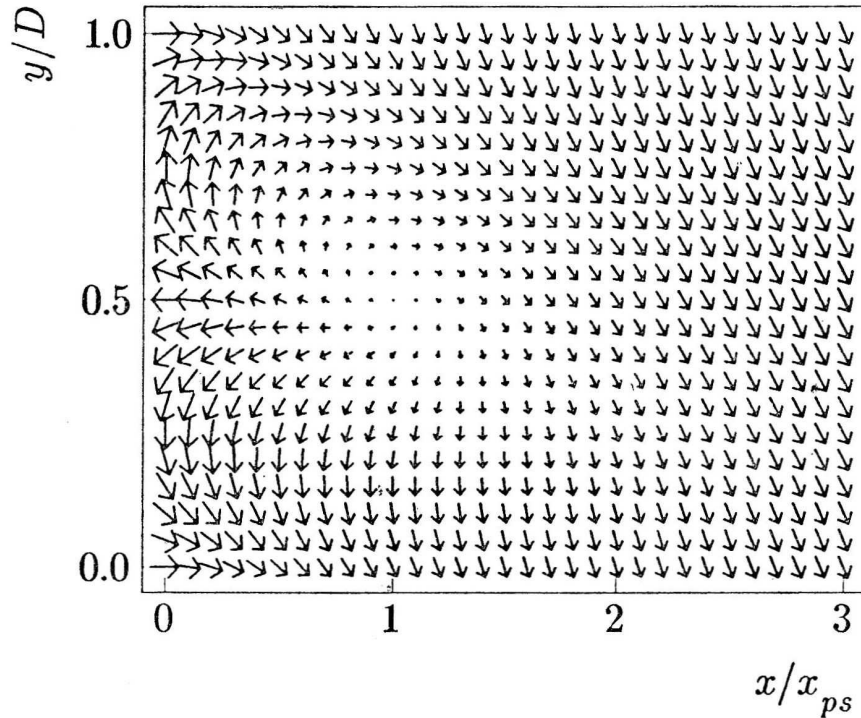
Thus in one PS period  $2\pi/E$ , each dislocation line crosses the width  $D$ , i.e. the train of dislocation lines sweeps the whole sample cross section.

In order to visualize the PS dislocation lines we show in Figs. 1 (a, b) the order parameter and the corresponding equiphase lines in the  $(x, y)$  plane for  $E = 10$  and  $Q = -0.5$  and for  $|\Delta_0|$  at the moment  $t_{ps}$  for which the PS lines cross the points  $(x_{ps}, y_{ps} = (2n + 1)D/2)$ . These figures are graphical presentations of the expressions for the CDW amplitude and phase

$$|\Delta(\mathbf{r}, t)|^2 = \left( \tanh \frac{x}{\sqrt{2}} \right)^2 + |\Delta_0|^2 e^{-2\beta x} + 2|\Delta_0| \tanh \frac{x}{\sqrt{2}} e^{-\beta x} \cos(\alpha x + Qy + Et),$$

$$\tan \Phi(\mathbf{r}, t) = \frac{-\tanh(x/\sqrt{2}) \sin Et + |\Delta_0| e^{-\beta x} \sin(\alpha x + Qy)}{\tanh(x/\sqrt{2}) \cos Et + |\Delta_0| e^{-\beta x} \cos(\alpha x + Qy)}, \quad (26)$$

respectively. One recognizes the typical vortex structure in the regions close to the point  $(x_{ps}, y_{ps})$ . Note that at these points the phase of the order parameter becomes undefined. The uniqueness of the solution is however preserved due to  $|\Delta(x_{ps}, y_{ps}, t_{ps})| = 0$ . Far from the dislocation lines, the vortex structure is deformed in order to accommodate to the periodicity in the  $y$ -direction and to the boundary conditions at  $x = 0$  and  $x \rightarrow \infty$ . Furthermore, by increasing  $x$ , the equiphase lines approach asymptotically the range of constant phase  $\Phi = Et_{ps}$ , determined by  $\Delta_R(x, t)$  from Eq. (10).



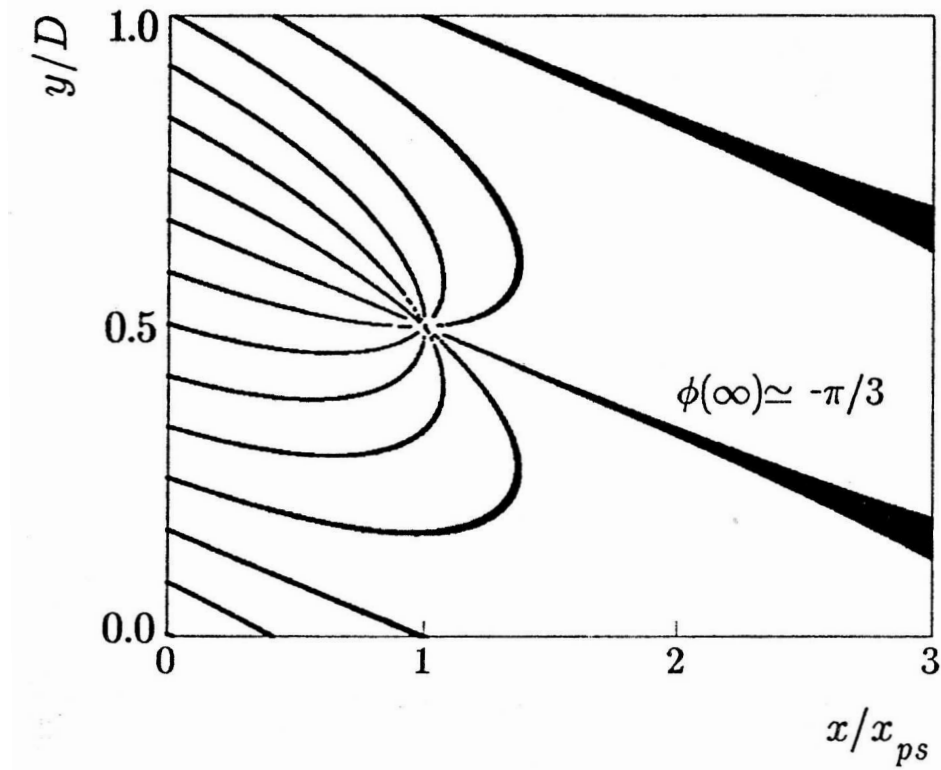


Fig. 1. (a, previous page) The order parameter  $\Delta(\mathbf{r}, t)$  (Eq. (26)) for  $E = 10$  and  $Q = -0.5$  and for  $|\Delta_0| = 1$ . The presented pattern repeats periodically on the  $y$ -axes. The characteristic  $x$  and  $y$  scales are  $x_{pj} = 0.49$  and  $D = 4\pi$  in reduced units, (b) The corresponding equiphase lines, marked in the intervals  $\pi/6$  starting from the value  $\Phi(x \rightarrow \infty) = \alpha x_{ps} \approx -\pi/3$ , and evaluated with the numerical precision  $\delta\Phi = 0.01$ .

A vortex structure presented in Fig. 1 remains qualitatively the same when  $Q$  and  $E$  vary. However, the characteristic scales  $x_{ps}$ , and  $D$ , and correspondingly the angle  $\theta$  between the equiphase lines and the boundary at  $x = 0$ , depend on  $Q$  and  $E$ . The latter is deduced from Eq. (26) in the limit  $x \rightarrow 0$ ,

$$\Phi(x \ll 1) \approx \alpha x + Qy. \quad (27)$$

The equation for the equiphase lines in this limit is thus

$$y = \frac{\Phi_0}{Q} - \frac{\alpha}{Q}x, \quad (28)$$

i.e.

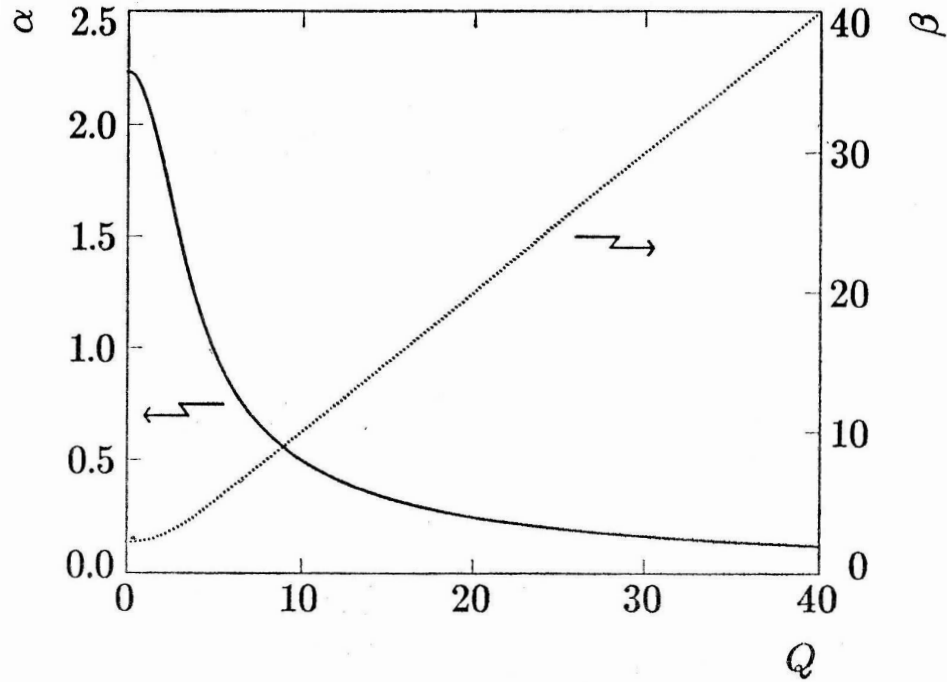
$$\tan \Theta \approx -\alpha/Q. \quad (29)$$

The dependence of  $\alpha$ ,  $\beta$ ,  $x_{ps}$  and  $\theta$  on the parameter  $Q$  for  $E = 10$  is shown in Fig. 2. It is evident that for  $Q = 0$ , i.e. for  $D \rightarrow \infty$ , the equiphase lines become parallel to the boundary. Simultaneously, the velocity of the dislocation lines  $v_y$  tends to infinity. This is the limit of planar PSs, realized by an instant sweep of the whole sample cross section by a single dislocation line.

In the opposite limit of large  $Q$ , i.e.  $D \rightarrow \infty$ , the equiphase lines become perpendicular to the boundary, the density of lines tends toward infinity, and  $v_y \rightarrow 0$ . In the picture of discrete chains, this limit corresponds to uncorrelated chains, with the PS process at each chain determined by a local boundary condition to which this chain is subjected.

The above conclusions become particularly important regarding the NBN amplitude. Taking into account that  $E \gg 1$ , one gets the periodic contribution to the voltage (6)

$$\begin{aligned} \delta V(t) = \sqrt{2} \lambda \left( 1 - \frac{8}{9} \varepsilon \right) A(Q, L_y) \frac{E}{Q^4 + E^2} \\ \times \left[ E \sin \left( Et + \frac{QL_y}{2} \right) + Q^2 \cos \left( Et + \frac{QL_y}{2} \right) \right]. \end{aligned} \quad (30)$$



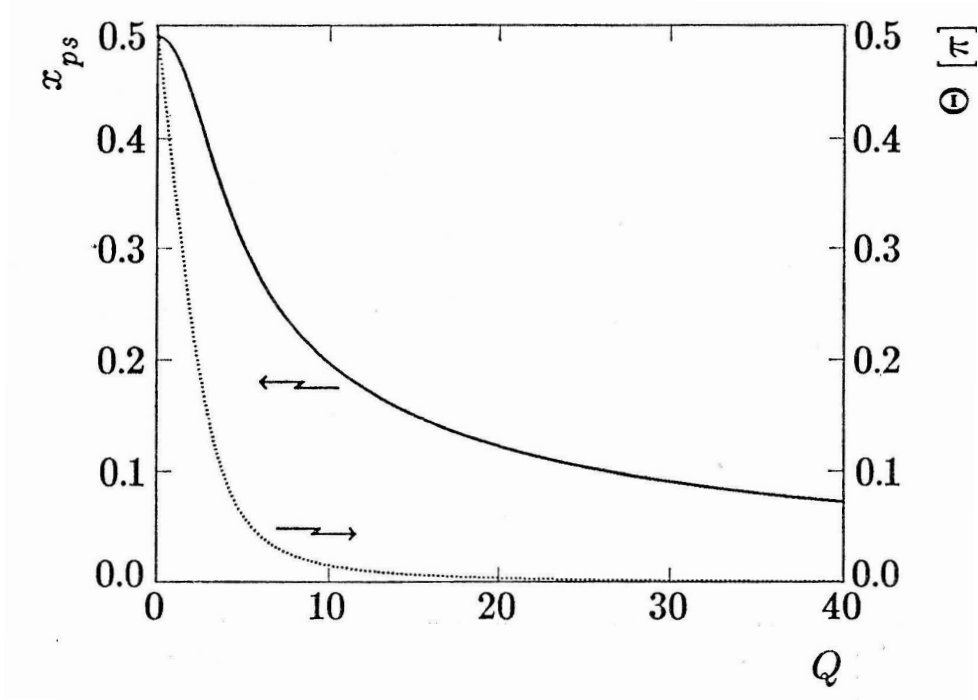


Fig. 2. (a, previous page) The dependence of  $\alpha$  and  $\beta$ , Eq. (20) on  $Q$  for  $E = 10$ . For  $Q = 0$ ,  $\alpha = \beta = \sqrt{E/2}$ . (b) The corresponding distance  $x_{ps}$  (Eq. (21a)) of the PS-plane from the boundary for  $|\Delta_0| = 1$ , and the angle  $\theta$  (Eq. (29)) of the equiphase lines  $\Phi(x \rightarrow 0) = \Phi_0$  with respect to the  $x$ -axes.

The amplitude

$$A(Q, L_y) = L_y L_z \frac{\sin(QL_y/2)}{QL_y/2}, \quad (31)$$

which results from the integration over the sample cross section  $S = L_y L_z$ , is sketched in Fig. 3. Note that  $A(QL_y \rightarrow 0) \rightarrow L_y L_z$ , i.e. the voltage (30) reduces in the limit of small  $Q$  to

$$\delta V(t) = \sqrt{2} \lambda \left(1 - \frac{8}{9} \varepsilon\right) L_y L_z \sin(Et), \quad (32)$$

i.e. to the expression corresponding to the planar regime. However, for  $L_y = 2n\pi$ , where  $n \neq 0$ , the overall voltage amplitude vanishes. These cases correspond to  $L_y = nD$ . The sample cross section consists of an integer number of bands of width  $D$ . Each of them contains full range of PS phases and does not

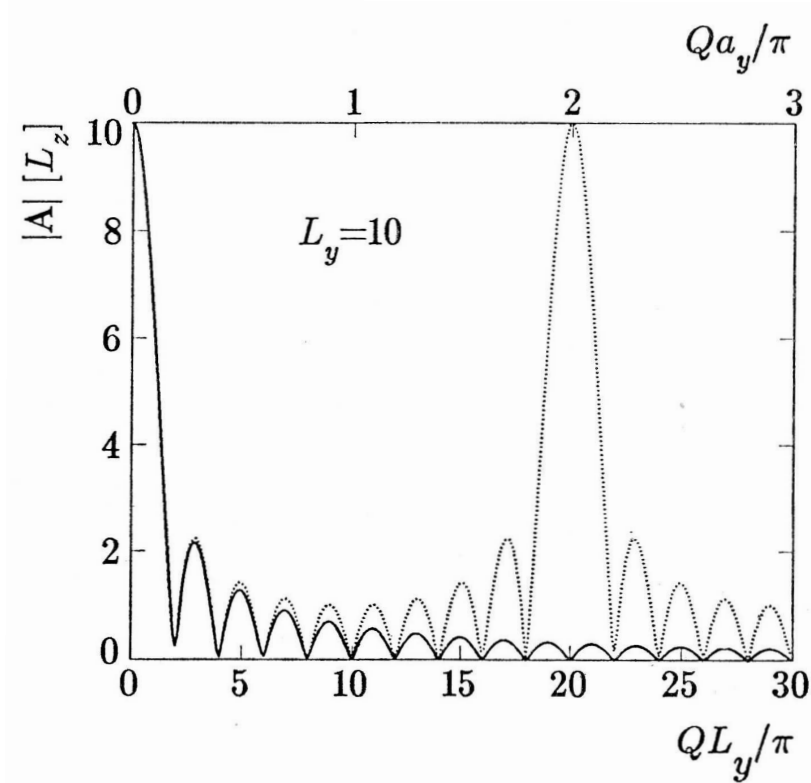


Fig. 3. The amplitude of the time dependent part of the voltage (30) in the continuous (Eq. (31), full line) and discrete (Eq. (34), dashed line) picture, for the system of width  $L_y = 10$ . The distance between the chains in the discrete case is assumed to be  $a_y = 1$ .

contribute to the voltage. The maxima in the voltage, on the contrary, correspond to  $L_y = (n+1/2)D$ . In fact, then only the band of width  $D/2$  contributes, since in it only the phases of the same sign participate. By increasing  $Q$ , i.e. by decreasing  $D$ , this contribution diminishes, so the voltage amplitude finally vanishes for  $Q \gg E$ .

The above result will be modified after taking into account the discrete chain structure. For a system consisting of  $N_y(N_z)$  chains at distance  $a_y$  ( $a_z$ ), the integration over the sample cross section is to be replaced by

$$\int dy \int dz \rightarrow L_y L_z \frac{1}{N_y} \sum_{n=0}^{N_y-1}, \quad (33)$$

where  $L_i = N_i a_i$  ( $i = y, z$ ) and  $n$  is the index of the chain at the position  $y_n = (n + 1/2)a_y$ . The voltage amplitude  $A$  then becomes

$$A(Q, L_y, a_y) = L_y L_z \frac{\sin(QL_y/2)}{N_y \sin(Qa_y/2)}. \quad (34)$$

As is evident from Fig. 3, the effect of sample discreteness is weak in the limit of small  $Q$ ,  $Q \ll a_y^{-1}$ . In particular, the amplitude (34) reduces to the expression (31) in the continuous limit  $a_y \rightarrow 0$ . However, for  $Q \geq a_y^{-1}$ , one encounters the effects of sample discreteness. We note in particular the case  $Qa_y = 2\pi$ , i. e.  $D = a_y$ . A dislocation line passes exactly from one chain to another in one PS period. In other words the PSs are again simultaneous throughout the sample cross section. Instead of the zero NBN amplitude, which one would expect in a continuous limit, we obtain again the planar result. Analogous reasoning holds also for  $Qa_y = 2k\pi$ , i.e.  $D = a_y/k$ , when the boundary conditions are again identical at all chains.

To conclude the above analysis, let us note that the sign of  $\Phi$  changes for  $Q \rightarrow -Q$ , as can be seen from the expression (26). This corresponds to the replacement of a vortex structure presented in Fig. 1. by the anti-vortex one. Simultaneously, the sign of  $v_y$  is reversed, i.e. the vortex and the anti-vortex travel in opposite directions (for the electric field  $E$  of a given sign). Similar conclusion holds for the  $x \rightarrow -x$  replacement. In our semi-infinite geometry the latter case corresponds to the effects of the barrier at the right end. Thus, with fixed  $Q$  and  $E$ , the PS generation at opposite boundaries proceeds through the generation of vortices and anti-vortices. Note that the sign of the electric field  $E$  alters the sign of the vortex (anti-vortex) velocity, but does not influence its topological structure.

## 5. Conclusions

The above analysis shows that the synchronization of PSs in front of a transversally extended barrier leads to the generation of dislocation lines with topological properties identical to those of static dislocation lines<sup>23)</sup>, i.e. vortices<sup>22)</sup>. The  $\mathbf{r}$ -dependences of phase and amplitude for the two types of dislocation lines however differ. In the case of dynamical dislocations, it follows from Eqs. (1) and (7) and is given by e.g. the expressions (26) and Fig. 1., while the static dislocation lines are usually presented as solutions of the Laplace equation for an elastic medium<sup>22)</sup>. The dynamics of dislocation lines in Fig. 1. is characterized by the PS diffusion in the longitudinal direction, and by mostly transverse motion and shape evolution which depends on the morphology of a barrier, i.e. on the corresponding boundary conditions for the CDW order parameter. This is to be compared with the usual inertial motion of dislocation lines in elastic media. The transverse motion of dynamic dislocation lines, Eqs. (15) and (23) is reflected in the relative shifts of the PS times at different points of the cross section. From the other side, the periodicity of the PSs at a given point of the cross section (i.e. at a given chain), and the corresponding periodicity of the NBN voltage, are not affected by the dynamics of dislocation lines.

Let us note that this conclusion is a direct consequence of the static behaviour of the order parameter close to the boundary. The previous one-dimensional results<sup>17)</sup> show that, due to the nonlinear effects the PS process becomes more and more localized to the PS centers by decreasing  $E$ . This suggests that the static approximation of the Eq. (1) close to the barrier and the subsequent conclusions are well founded

in particular in the physical range of the electrical fields ( $E \ll 1$ ). From the other side, our results show that, while the boundary condition change the spatial scales for the PS process, they do not change qualitatively its dynamical properties. The above results are therefore expected to remain qualitatively the same in the physical limit of small electric field ( $E \ll 1$ ), the only exception being the sinusoidal voltage which should be replaced by a multiharmonic one.

The motion of the dislocation lines is directly reflected also in the overall NBN amplitude of the sample, which is in general reduced with respect to the planar regime of simultaneous PSs. The periodic boundary condition, analyzed in detail in Sect. 4, shows that the NBN amplitude may even vanish in some special circumstances. Such boundary condition is presumably too idealized and never achieved in real samples. More realistically, the boundary conditions vary stochastically across the boundary. Moreover, generally the barrier is not flat, i.e. its position as well can vary transversally. Both effects would lead to a statistical distribution of the PS positions and, more important, of the relative moments of the PSs at different chains. The NBN amplitude will then be roughly proportional to  $\sqrt{L_y L_z}$ , instead of the  $L_y L_z$ -law obtained in a planar regime.

Finally, the transverse motion of dislocation lines is not expected to be the reason of the finite widths of the NBN spectral lines and the associated low frequency peaks in the experimental voltage spectra. The temporal variations of the order parameter in the regions of obstacles, neglected in our approach, may be at most responsible for very slow temporal variations in the NBN amplitude, observed in some experiments<sup>6)</sup>. More likely however, both effects are to be associated with the longitudinal and/or transversal variations of the external electric field, irregular sample cross-sections and/or inhomogeneities in the weak impurity concentrations, discussed in detail in Ref. 20.

#### References

- 1) R. E. Peierls, Ann. Phys. **4** (1930), 121; *Quantum Theory of Solids*, p. 108, Oxford University Press (1955);
- 2) H. Fröhlich, Proc. Royal Soc. A **223** (1954) 296;
- 3) For a general review see e. g. P. Monceau, *Electronic Properties of Inorganic Quasi One-Dimensional Materials II*, p. 139, Edited by P. Monceau, Riedel, Dordrecht (1985); G. Grüner, Rev. Mod. Phys. **60** (1988) 1129;
- 4) L. Mihaly and G. X. Tessema, Phys. Rev. B **33** (1986) 5858; G. Mihaly and P. Beauchene, Solid State Comm. **63** (1987) 911;
- 5) J. W. Lyding, J. S. Hubacek, G. Gammie and R. E. Thorne, Phys. Rev. B **33** (1986) 4341;
- 6) B. Bhattacharya, J. P. Stokes, M. J. Higgins and R. A. Klem, Phys. Rev. Lett. **59** (1987) 1849;
- 7) see e. g. A. Bjeliš, *Low Dimensional Conductors and Superconductors*, p. 409, Ed. D. Jérôme and L. G. Caron, Plenum Press (1987) and references therein;
- 8) H. Fykyama and P. A. Lee, Phys. Rev. B **17** (1978) 535;
- 9) P. A. Lee and T. M. Rice, Phys. Rev. B **19** (1979) 3970;



- 10) P. Monceau, J. Richard and M. Renard, Phys. Rev. B **25** (1982) 918; Phys. Rev. B **25** (1982) 931;
- 11) G. Grüner, A. Zawadowski and P. M. Chaikin, Phys. Rev. Lett. **45** (1981) 511;
- 12) L. Sneddon, M. C. Cross and D. S. Fisher, Phys. Rev. Lett. **49** (1982) 292;
- 13) S. N. Coppersmith and P. B. Littlewood, Phys. Rev. Lett. **57** (1986) 1927; Phys. Rev. B **31** (1985) 4049;
- 14) L. P. Gor'kov, Pis'ma Zh. Eksp. Teor. Fiz. **38** (1983) 76 (Sov. Phys. – JETP Lett. **38** (1983) 87); L. P. Gor'kov, Zh. eksp. Teor. Fiz. **86** (1984) 1818 (Sov. Phys. – JETP **59** (1985) 1957);
- 15) J. S. Langer and V. Ambegaokar Phys. Rev. **164** (1967);
- 16) B. I. Ivlev and N. B. Kopnin, Pis'ma Zh. Eksp. Teor. Fiz. **28** (1978) 640 (Sov. Phys. – JETP Lett. **28** (1978) 592); B. I. Ivlev and N. B. Kopnin, J. Low Temp. Phys. **44** (1980) 453;
- 17) I. Batistić, A. Bjeliš and L. P. Gor'kov, J. Physique **45** (1984) 1049;
- 18) A. Bjeliš and D. Jelčić, J. Physique Lett. **46** (1985) 293;
- 19) D. Jelčić, A. Bjeliš and I. Batistić, Phys. Rev. B **38** (1988) 4045;
- 20) D. Jelčić and A. Bjeliš, Phys. Rev. B **43** (1991) 1735;
- 21) S. N. Artemenko, A. F. Volkov and A. N. Kruglov, Zh. Eksp. Teor. Fiz. **91** (1987) 1536 (Sov. Phys. – JETP **64** (1987) 906);
- 22) N. P. Ong and K. Maki, Phys. Rev. B **32** (1985) 6582;
- 23) D. Feinberg and J. Friedel, J. Physique **49** (1988) 485;
- 24) A. Bjeliš, Physica Scripta T **29** (1989) 62;
- 25) A. Bjeliš, *Applications of Statistical and Field Theory Methods to Condensed Matter*, p. 325, edited by D. Baeriswyl, A. R. Bishop and J. Carmelo, Plenum Press, New York (1990).

DINAMIČKE DISLOKACIONE LINIJE U SISTEMIMA S VALOVIMA  
GUSTOĆE NABOJA

DAJANA JELČIĆ and ALEKSA BJELIŠ

*Fizički odjel Prirodoslovno-matematičkog fakulteta, Sveučilišta u Zagrebu, P.O.B. 162,  
41001 Zagreb, Hrvatska*

UDK 538.91

Originalni znanstveni rad

Razmatrana su topološka svojstva konverzije kolektivne struje nošene valom gustoće naboja u omsku struju ispred barijere koja u potpunosti zaustavlja kolektivni transport. U okviru Gor'kovljevog modela se pokazuje da centri istovremenih proklizavanja faze formiraju familiju dislokacionih linija. Oblik i dinamika dislokacionih linija ovise o morfologiji barijere. Takva ovisnost odražava se u amplitudi uskopo-jasnog šuma, ali ne utječe na njegovu frekvenciju.